Journal of Power Sources, Volume 372, 2017, Pages 245-251
DOI:10.1016/j.jpowsour.2017.10.078

Self-Balancing Feature of Lithium-Sulfur Batteries

V. Knap[a], D.-I. Stroe[a], A. E. Christensen[b], K. Propp[c], A. Fotouhi[c], D. J. Auger[c], E. Schaltz[a], R. Teodorescu[a]

[a] Department of Energy Technology, Aalborg University, Aalborg, 9000, Denmark

[b] Lithium Balance A/S, Hassellunden 13, Smørum, 2765 Denmark

[c] Advanced Vehicle Engineering Centre , Cranfield University, Bedfordshire MK43 0AL, UK

The Li-S batteries are a prospective battery technology, which despite to its currently remaining drawbacks offers useable performance and interesting features. The polysulfide shuttle mechanism, a characteristic phenomenon for the Li-S batteries, causes a significant self-discharge at higher state-of-charge (SOC) levels, which leads to the energy dissipation of cells with higher charge. In an operation of series-connected Li-S cells, the shuttle mechanism results into a self-balancing effect which is studied here. A model for prediction of the self-balancing effect is proposed in this work and it is validated by experiments. Our results confirm the self-balancing feature of Li-S cells and illustrate their dependence on various conditions such as temperature, charging limits and idling time at high SOC.

Keywords: inherent balancing, lithium-sulfur battery, self-discharge, series-connected batteries

Published by Elsevier. This is the Author Accepted Manuscript issued with: Creative Commons Attribution Non-Commercial No Derivatives License (CC:BY:NC:ND 4.0).
The final published version (version of record) is available online at DOI:10.1016/j.jpowsour.2017.10.078. Please refer to any applicable publisher terms of use.

1. Introduction

Lithium-Sulfur (Li-S) battery is a prospective battery chemistry for current and future applications. Nowadays, their specific energy has reached 160–350 Wh/kg, with a prospect to accomplish 500–600 Wh/kg, which gives them an advantage above the widely used Lithium-ion (Li-ion) batteries with specific energy of 140–240 Wh/kg. Moreover, in a long-range their cost is expected to be lower than that of Li-ion batteries due to the use of less expensive active materials. However, as they are not a mature battery technology, there are several drawbacks, which have to be addressed either from the cell assembly or battery application point of view; i.e. fast capacity fade, shuttle phenomenon leading to high and quick self-discharge, solubility of active species and complex charge and discharge characteristics. [1], [2]

From the battery balancing perspective, one can see that it is an essential part of battery operation, as it has high impact on safety, amount of available capacity and battery lifetime. A proper balancing scheme primarily helps to achieve most energy per use, but also prevent states such as over-charging, over-discharging or thermal runaway, which may lead to dangerous situations. Furthermore, when cells with various state-of-charge (SOC) levels are present in a series connection, the battery pack operation is limited by the cell with the highest (charging) or the lowest (discharging) SOC, as illustrated in Fig. 1 a). Moreover, ageing phenomena are often related to cell potential, SOC level or temperature, which might vary at unbalanced cells and consequently cause non-uninform degradation, which might result in cell premature failing. [3], [4], [5]

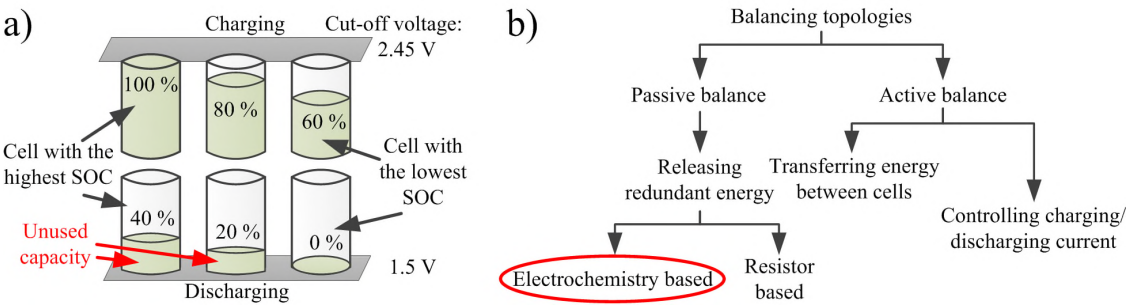

Figure 1. a) Illustration of the cells with an unbalanced state-of-charge and consequently resulting an unused capacity. Voltage levels are typical for cycling of Li-S cells. b) Classification of typical balancing methods, together with the proposed electrochemistry based method.

Balancing methods are typically classified into passive or active. The passive methods rely on dissipating the excess energy, which is usually done through a shunt resistor. This solution is simple and low cost, but may not be sufficient for applications with very strict energy use. Active methods rely on transferring energy between cells or controlling flowing current. They have usually higher efficiency and speed of balancing than the passive methods; however additional power electronic elements and controls are needed, which increase the complexity and cost of the solution. [3], [4], [5], [6], [7]

Li-S, being a complex solution based chemistry, introduces a new type of passive dissipative balancing method, which is electrochemistry-based. A classification of balancing methods is shown in Fig. 1 b), together with this new concept. Polysulfide shuttle mechanism, which is present in Li-S batteries, and explained in detail in [8] and [9], introduces high self-discharge, especially at high SOC levels. This inherent self-discharge process can be utilized for dissipating the energy of the unbalanced cells with

higher charge. Therefore, by the adequate operation, the Li-S cells can be fully or at least partially self-balanced without any additional switches.

In order to demonstrate the self-balancing ability of a Li-S cell, the cell is modelled including the self-discharge behavior, which is caused by the polysulfide shuttle. The simulations are performed for three cells connected in series in order to evaluate the self-balancing capability at various conditions. Afterwards, the model and the self-discharge capability are validated by experimental tests conducted on 3.4 Ah Li-S pouch cells and the usability of the self-balancing is discussed.

The paper is structured as follows: In the second section – Methodology, the laboratory experiment is described, together with the quantification methods for evaluating the cell balancing. The third section describes the modelling of the single Li-S cell and also the general simulation platform and the fourth section presents the simulation results for various conditions. The experimental results are shown and discussed in Section 5 and the discussion related to the self-balancing capability and its practical implementation is in Section 6.

2. Methodology

Three Li-S cells (labelled S1, S2, S3) connected in series are tested in order to evaluate the balancing. The cells are unbalanced by setting their initial SOC to 0, 10 and 20 %, respectively. The cells are cycled five times at 0.34 A (0.1 C-rate) for charging with various cut-off limits and 0.68 A (0.2 C-rate) for discharging to the 1.5 V. These currents are considered as the nominal currents for the cell.

2.1 Laboratory experiment

The cells used for the laboratory experiment were 3.4 Ah Li-S long-life type cells from OXIS Energy. They consist of a carbon/sulfur composite cathode, a lithium foil anode, organic solvent and polymeric separator. The cells were individually characterized using a Digatron BTS 600 battery test station and they were cycled in series using a FuelCon Evaluator B Battery Test Station, illustrated in Fig. 2 a). Only the nominal currents were always applied to the cells, except during constant voltage charging mode, when the charging current was reduced. The typical 'nominal' cycle is composed from the charge and the discharge. The charge has 2.45 V or 11 hours cut-off limits, whatever is reached first, and then the cell is considered fully charged. The discharge has 1.5 V cut-off limit, when the cell is considered fully discharged.

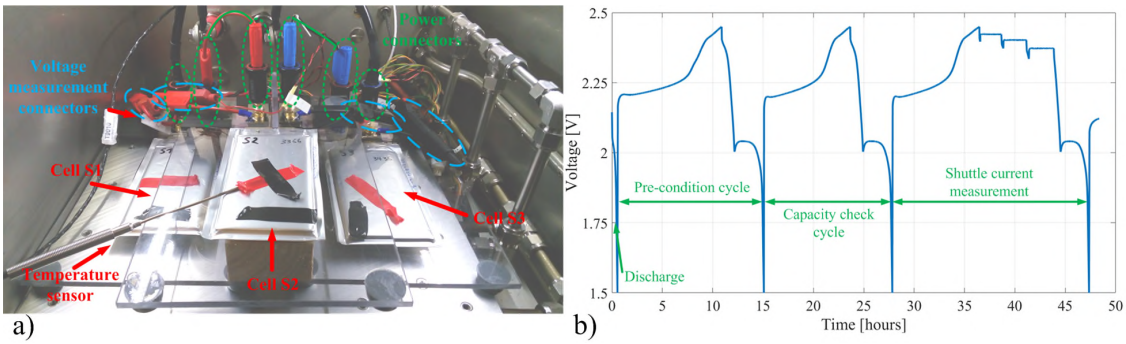

Figure 2. a) Three Li-S cells connected in series during cycling at FuelCon Evaluator B Battery Test Station. From left to right is cell S1, S2 and S3. b) The voltage profile from the 5th round of the characterization tests at cell S1.

The individual characterization consisted of discharging the cell to obtain the information about the remaining charge from the previous cycling, a pre-conditioning cycle [10], a cycle to obtain the actual capacity of the cell, the direct shuttle current measurement [10] and a cycle to discharge the cell to a pre-determined SOC level. For the experimental tests, the SOC was computed according to (1),

$$\mathrm{SOC} = Q_{\mathrm{meas}} / Q_{\mathrm{cap}} \tag{1}$$

where Q_{cap} is the capacity obtained from the capacity check cycle and Q_{meas} is:

a) the measured discharged capacity obtained during the first discharge step, when the voltage reached the discharging cut-off limit of 1.5 V,

b) the discharged amount of ampere-hours to reach the target SOC during the cycle for setting the SOC (after the cell being fully charged), computed as $Q_{\mathrm{meas}}=0.9\cdot Q_{\mathrm{cap}}$ and $Q_{\mathrm{meas}}=0.8\cdot Q_{\mathrm{cap}}$ for the remaining 10 % and 20 % of SOC, respectively.

The specific composition of the characterization for each round is shown in Table I. The voltage profile from the 5$^{\mathrm{th}}$ round of the characterization tests is illustrated in Fig. 2 b) for cell S1.

TABLE I. Specific content of the characterization tests.

Characterization rounds		
1.	**2. – 4.**	**5.**
Discharge	Discharge	Discharge
Pre-condition cycle	Pre-condition cycle	Pre-condition cycle
Pre-condition cycle	Capacity check cycle	Capacity check cycle
Capacity check cycle	Cycle for setting the SOC	Shuttle current measurement
Shuttle current measurement		
Cycle for setting the SOC		

During the cycling of the cells connected in series, the voltage of each cell was monitored, together with the current flowing through the cell string and temperature measured on the middle cell S2. The performed experiments together with their charging cut-off limit are illustrated in Fig. 3. The term 'balanced cells' means that all the cells were individually discharged to 0 % SOC at the previous characterization test. The term 'unbalanced cells' means that the cells were discharged at the previous characterization test to 0, 10 and 20 % SOC for cell S1, S2 and S3, respectively. A cycle for cycling the series-connected cells consisted of a charging and a discharging step. Each step (charge/discharge) was completed when the cut-off limits were reached by at least one of the cells. The discharging cut-off limit was always 1.5 V. The cells were subjected to five consecutive charging – discharging cycles.

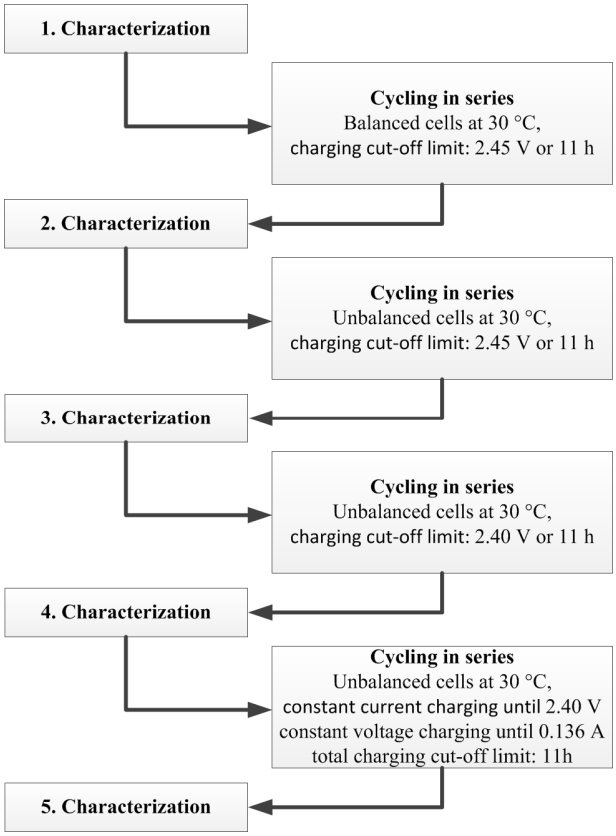

Figure 3. Test scheme.

2.2 Quantification and evaluation of balancing

In order to compare and evaluate specific balancing strategies, it is necessary to quantify their performance. For this purpose, we have selected the three following metrics. The maximum difference between the cells in SOC is represented by max ΔSOC. The performance of the series-connected cells in terms of 'useful' capacity is expressed by the throughput discharge capacity. Furthermore, an extent of the unified behavior of the cells is quantified as a dissimilarity of voltage discharging curves.

2.2.1 Maximum difference in SOC (*max ΔSOC*). The *max ΔSOC* is computed as the difference between the cell with the highest SOC and the cell with the lowest SOC. In the beginning of the balancing test, the maximum difference in SOC between the cells is *max ΔSOC* = 20 %. The ideally balanced cells in terms of SOC would have *max ΔSOC* = 0 %. In the simulations it is possible to track the SOC all the time, the value taken into account to compute *max ΔSOC* is always at the end of discharge. For the laboratory experiment, it is possible to directly evaluate the SOC only before and after cycling during the individual characterization of the cells.

2.2.2 Throughput discharge capacity (*TDC*). Due to the series-connection approach, the discharging capacity of the battery string is limited by the cell with the lowest SOC as it reaches the voltage cut-off limit the earliest, which results into the unused capacity in other cells (illustrated in Fig. 1 a)). Therefore, the balancing leads to the improved *TDC* of the battery string. For continuous discharge during one cycle, *TDC* is computed as integration of the load current (I_L) from the beginning of discharge (*t_bod*) until the end of discharge (*t_eod*).

$$TDC = \int_{t_bod}^{t_eod} |I_L / 3600| \, dt \qquad (2)$$

2.2.3 Dissimilarity of the discharging curves (*DDC*). The uniformity of cells behavior is another aspect, which should be considered, while dealing with balancing. The cells that do not behave similarly might lead to exposure to different mechanisms, which can further deteriorate the cells performance and lifetime. More specifically for the Li-S batteries, it can lead to different exposure of shuttling or precipitation of Li_2S. The ideal

DDC has a value equal to zero, meaning the cells behave completely identical. The DDC is computed as follows:

$$V_{\text{mean}}(\text{t}) = (V_{\text{S1}} + V_{\text{S2}} + \cdots + V_{\text{S}n}) / n \quad (3)$$

$$\text{DDC} = (\sum_1^n |V_{\text{mean}}(t) - V_{\text{S}i}(t)|) / n \quad (4)$$

Where $V_{\text{mean}}(t)$ is the average voltage curve for the cells 1 to n and $V_{\text{S}i}$ stands for an i-th cell voltage curve.

3. Modelling

3.1 Battery module model

The structure of the battery module model, including cells' connection and illustrated signals, is shown in Fig. 4 a). It consists of the current control unit (CCU) and three cells connected in series in a homogenous temperature environment. The CCU provides the current, which flows through all cells and it also receives the information about SOC and voltage from each cell.

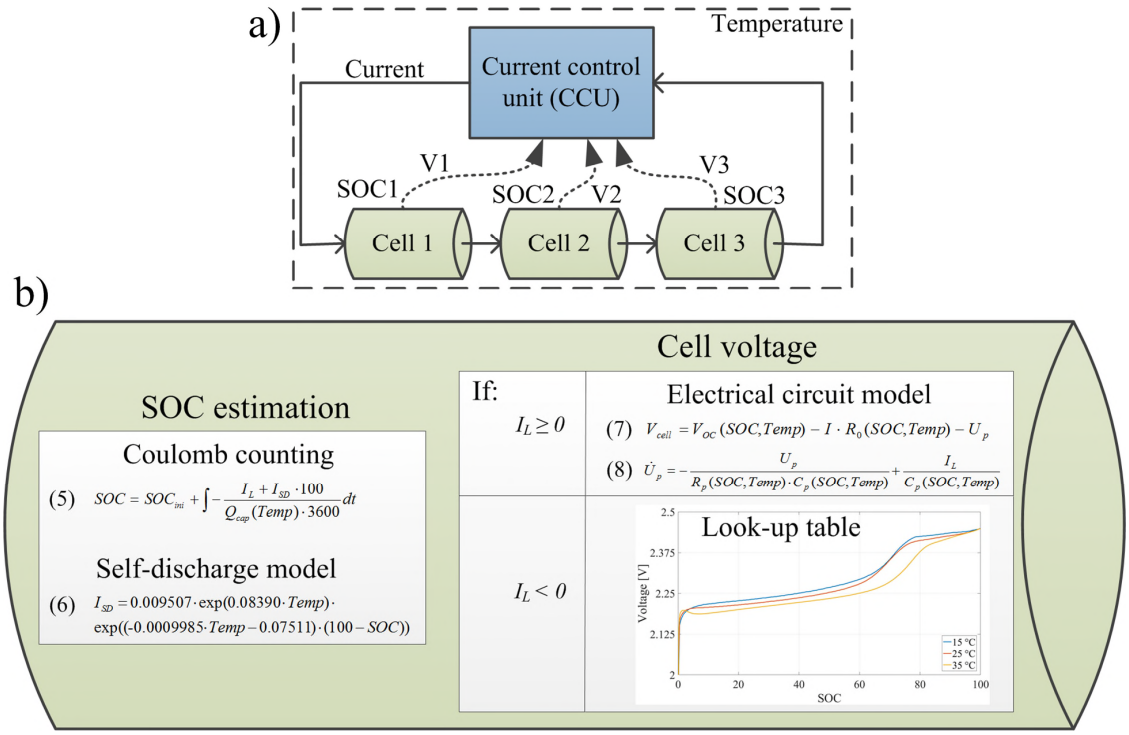

Figure 4. a) Battery module model with shown connection of the cells and marked signals and inputs. b) Li-S battery cell model, illustrating SOC counting according to Coulomb counting method and the self-discharge model. The cell's voltage is determined for relaxation and discharge operation modes based on the equivalent circuit discharge model [11], while for charging mode is based on experimentally derived look-up tables.

3.2 Li-S battery cell model

The structure of the Li-S cell model is illustrated in Fig. 4 b). During charging (negative I_L), the voltage provided by the model is obtained from look-up tables based on experimental measurements, dependent on SOC and temperature (*Temp*). For discharging (positive I_L) and relaxation (I_L = 0), the voltage is provided by the multi-temperature state-dependent equivalent circuit discharge model for Li-S batteries presented in [11].

The SOC in the model is computed by coulomb counting, including the self-discharge model of Li-S batteries based on direct shuttle current measurement presented in [12]. The total capacity (Q_{cap}) for coulomb counting is implemented as a look-up table dependent on temperature.

3.3 Current Control Unit

The CCU provides the current based on the user specifications. In this work, the current is limited only to its nominal values, which are 0.34 A (0.1 C-rate) for charging and 0.68 A (0.2 C-rate) for discharging The SOC, voltage and time are used for the control of the battery operation (charging/discharging/relaxation).

3.4 Determination of look-up table values

The values for Q_{cap} and charging voltage are determined from laboratory measurements. During the experiment at a single temperature, the cell was cycled two times by 0.34 A charging (to 2.45 V or 11 hours) and 0.68 discharging (to 1.5 V). This test was performed for three temperatures: 15, 25 and 35 °C. The charging and discharging capacity during the second cycle were recorded. These capacities were corrected by the self-discharged amount according to [12], by adding the DCH/CHA lost capacity due to the self-discharge to DCH/CHA measured capacity and by that obtain the DCH/CHA total capacity. The total capacity Q_{cap} was taken as an average value between the corrected charging and discharging capacity. Their values are presented in Table II. The charging voltage profiles as a function of SOC are shown in Fig. 4 b).

TABLE II. Measured and corrected capacity values due to the self-discharge.

Temp [°C]	DCH capacity measured [Ah]	Capacity lost by self-discharge [Ah]	Total DCH capacity [Ah]	CHA capacity measured [Ah]	Additional capacity due to self-discharge [Ah]	Total CHA capacity [Ah]	Average capacity [Ah]
15	2.5590	0.0140	2.5730	2.6750	0.0150	2.6600	2.6165
25	2.6970	0.0307	2.7277	2.8270	0.0342	2.7928	2.7603
35	3.5050	0.0839	3.5889	3.6400	0.1012	3.5388	3.5639

4. Simulation studies of ideal cells

The simulations studies were performed for three ideal (identical) cells connected in series. At first, the effect of charging voltage cut-off was studied by varying the cut-off limit to 2.35, 2.40 and 2.45 V. In the second study case, a relaxation period was introduced after the first reaching of the cut-off limit and an additional charging step was inserted. The effect of temperature on balancing was studied in the third study case. The results are graphically summarized in Fig. 5. The measured values are linearly fitted to obtain the slope of the curves. For the DDC graphs an ‘error bar’ is also plotted to present the mean, maximum and minimum values for the cell curves.

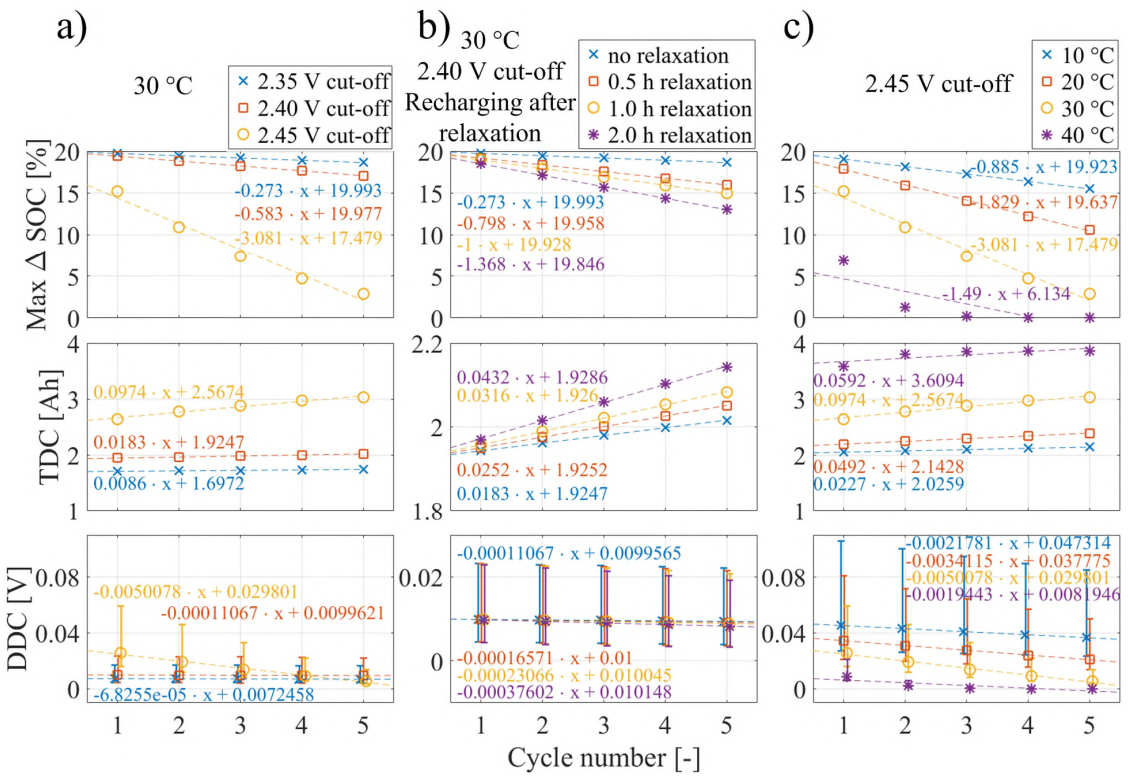

Figure 5. Simulation results from five cycles at three ideal cells connected in series, *x* stands for number of cycles. a) cycling at 30 °C to various charging cut-off limits; b) cycling at 30 °C to 2.40 V, followed by various relaxation periods and repeatedly charged to 2.40 V before the discharge; c) cycling at various temperature levels to 2.45 V charging voltage limit.

The voltage cut-off limits determines how much the cells are going to be charged. For a higher limit (2.45 V), a cell will enter and stay in the shuttling region, which helps in the balancing. From Fig. 5 a), it can be observed that allowing the cells to be charged until 2.45 V has a great impact on the balancing; already after the first cycle *max ΔSOC* is reduced by almost 5 % and after five cycles, the final *max ΔSOC* is 2.88 %. The balancing capability is reduced with lowering the voltage cut-off limits to 2.40 and 2.35

V, but it is still present. A similar trend is observable also for the *TDC* and *DDC*. For a 2.45 V cut-off limit, the *DDC* is the highest in the beginning, because there is the largest difference between the discharging voltage curves due to the character of the Li-S high voltage plateau. Nevertheless, during cycling the *DDC* is highly improved to again outperform the lower voltage cut-off limits.

The next study case was focused on the effect of the relaxation time on the self-balancing. In this case the cells were kept for a prolonged time at high SOC. When the cell was charged, it was left idling for a certain period of time and then was charged again to the charging cut-off limits before the discharge step. By doing so, the cell is left longer time at the maximum allowed SOC by charging and by that it is exposed more to the shuttling. The results presented in Fig. 5 b) were obtained for a 2.40 V charging cut-off limit and are showing that with increased relaxation time at high SOC, the cell balancing is improved.

In the next study case, different temperature levels were investigated, because the shuttle current is highly dependent on temperature [12]. This behavior was expected to be reflected also into the balancing capabilities of the cell. The higher the temperature of the cells is, the faster the balancing is over the cycling, as illustrated in Fig. 5 c). There is also a noticeable change of relatively linear trend of *max ΔSOC* during the 10–30 °C interval into rather exponential for 40 °C due to rapid balancing already at the first and the second cycle.

5. Experimental results

The capacity values of the cells S1, S2 and S3, which were obtained during the first characterization test, are 2.933, 2.954 and 2.818 Ah, respectively. Consequently, it can be observed that the cells were already partially aged. In order to fairly evaluate the balancing capabilities, at first we needed to see how the behavior of the cells is when they are cycled as initially balanced (discharged to 1.5 V, which represents 0 % SOC). The comparison of the balanced and unbalanced cells cycled at 30 °C to 2.45 V is shown in Fig. 6. It is noticeable that for both cases, there was a remaining charge in the cells between 0.295 and 0.402 Ah, which translated to SOC represents 11–14 %; this behavior is caused by the presence of a relaxation period before every characterization test. These results are in agreement with the additional discharging capacity obtained by introducing a relaxation period after the first discharge, reported by Zhang et al. [13]. Zhang et al. explain this behavior of discharging capacity by active polysulfides moving to and being trapped in the separator due to their effort of sustaining charge equilibrium throughout the cell. The charge equilibrium is being disturbed at first place by the Li+ cations being too slowly transported to the cathode during discharge. Afterward, during the relaxation period these trapped polysulfides diffuse back into the cathode. The cell model implemented in our work is not able to reproduce this behavior. Therefore, the SOC results remain only as a predictive indicator, but they are not closely matching the experimental results. From the $max\,\Delta SOC$ metric, it is seen that the initially balanced system has a $max\,\Delta SOC$ slightly, but neglectably higher than the unbalanced system. In the balanced system, the *TDC* is high and nearly constant, while the unbalanced system shows a highly reduced *TDC* in the beginning which is improved during the cycling. A

similar trend is observable in the *DDC*. Even though the cells are not identical, the mean *DDC* is nearly constant for the balanced system, while it has initially a high value for the unbalanced system and over the cycling it gets closer to the balanced system. Moreover, the voltage profile during the first and the last cycle of the unbalanced system is shown in Fig. 7 to demonstrate the increased capacity and more uniform behavior of the cells after cycling. Thus, the self-balancing ability of the Li-S cells was experimentally verified.

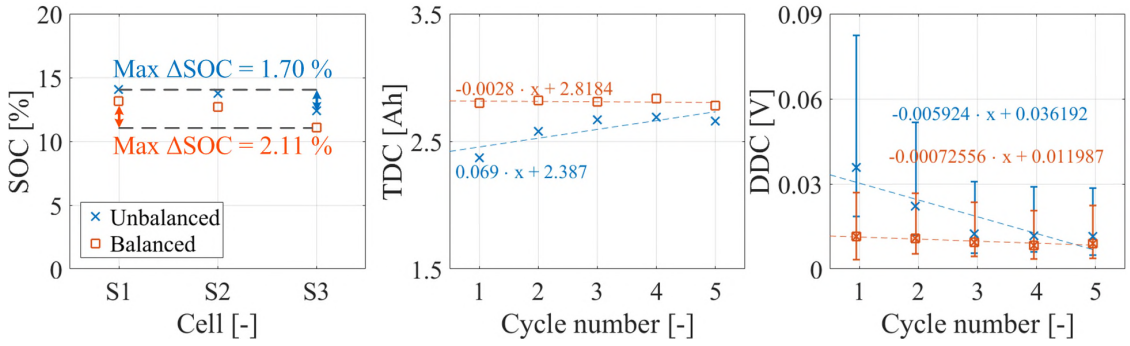

Figure 6. Comparison of experimental results for the cells initially balanced and unbalanced, cycled at 30 °C with charging cut-off of 2.45 V, *x* stands for number of cycles.

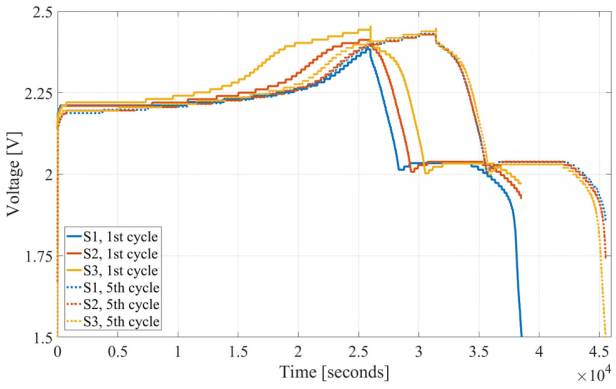

Figure 7. The first and the last cycle of the series cell cycling at 30 °C to 2.45 V.

The next step was to verify the model validity and to experimentally obtain the cell balancing capability at different conditions. The comparison of experimental and simulation results is shown in Fig. 8. For the comparison to the experimental test of charging to 2.40 V by constant current and constant voltage charging to 0.136 A was selected the simulation scenario with charging to 2.40 V, 0.5 h relaxation period, followed by recharging again to 2.40 V. This simulation scenario was selected based on the time spent for relaxation and recharging was the closest to the length of the constant voltage charging. The implemented model does not support constant voltage charging mode. It is important to note that the simulations were performed for the 'ideal' identical cell model. For the cycling with charging up to 2.45 V, the simulation and experimental results are closely matching. For the charging up to 2.40 V, or charging up to 2.40 V with relaxation and recharging or constant voltage charging, one can see that the predicted $max\ \Delta SOC$ do not match. The reason for it is most probably the recovery of discharging capacity due to transport limitations, as explained earlier. However, the *TDC* simulation results are very close to the experimental results and they have similar trend. The *DDC* results show very accurate match for case of charging to 2.45 V. However, for charging to 2.40 V the slope differs by one or nearly two orders between the simulation and experimental results, though the improving trend in the *DDC* is alike. Therefore, we can conclude that the implemented model can be used for predicting the balancing of Li-S cells due to the shuttle current. The *TDC* is provided with a high accuracy, while the *DDC* accuracy can vary according to the charging conditions. The SOC balancing represents more complex challenge and it is necessary to include the SOC/capacity recovered during the relaxation periods or different way of the SOC estimation.

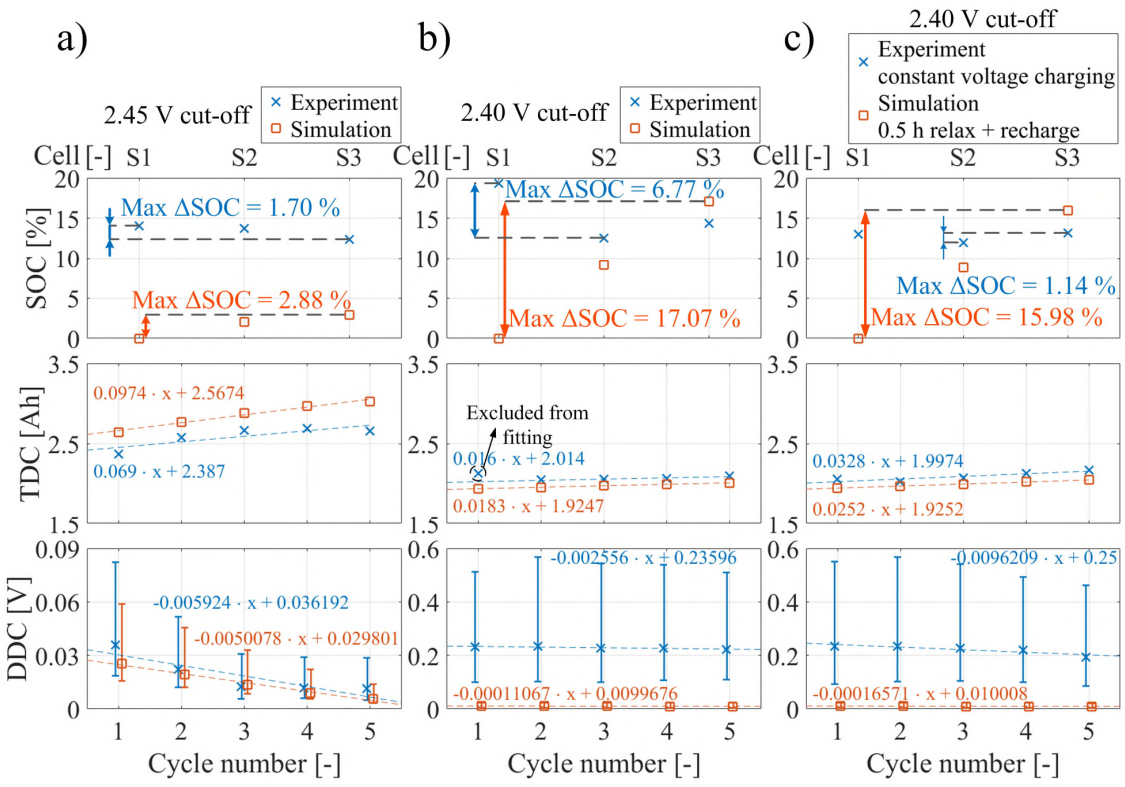

Figure 8. Comparison of experimental and simulation results, *x* stands for number of cycles. a) cycling to 2.45 V cut-off limit, b) cycling to 2.40 V cut-off limit, c) charging to 2.40 V cut-off limit and followed by constant voltage charging mode in the case of experiment or by relaxation for 0.5 hour and repeatedly charging to 2.40 V in the case of simulation.

6. Discussion

The self-balancing feature of the Li-S batteries opens new possibilities to reduce the amount of power electronic parts of the system and by that increase the reliability and reduce the cost, or to enhance standard balancing strategies. In a practical application, in order to extend the lifetime, the charging cut-off limit of the Li-S batteries is expected to

be reduced and to be lower than 2.45 V. It was demonstrated that even with the lower charging cut-off limit of 2.35 V, the cells are able to slowly balance themselves. To take advantage of both benefits, the longer lifetime during the limited charging operation, and the rapid balancing, there can be implemented two modes of operation. The first mode would be the normal operation with reduced charging cut-off limits. The second mode would be balancing, which would try to boost the Li-S cells balancing capability. This can be obtained by changing one or several factors: increase of temperature, increase of charging cut-off limits and increase the time spent at the high voltage plateau (the higher the better). Also the constant voltage charging at the high voltage plateau can be beneficial, but it is important to consider safety in terms of cells' heating [8] and gassing [14], and also possible degradation of the cells. Generally, the degradation of the Li-S cells is a remaining question, as it is not clear how much will the cells aged at various self-balancing conditions.

7. Conclusions

The Li-S battery is a prospective technology, which despite to its currently remaining drawbacks offers useable performance and interesting features. In this work, the self-balancing feature of Li-S cells was investigated and modelled. At the higher SOC levels (approximately above 70 %, at the high voltage plateau), the significant self-discharge takes place, because of the polysulfide shuttle mechanism. This self-discharge during the operation of the series-connected cells results gradually in their SOC equalization due to the energy dissipation at the higher-charged cells. The self-balancing rate can be controlled and influenced by adjustment of the conditions as temperature, charging cut-off limits and time spent at the high voltage plateau. Implications of this

self-balancing feature could be simplification or complete exclusion of electronic circuits dedicated for balancing, which would result into cost reduction of battery packs and reliability increase by omitting possibly failing parts. For the self-balancing prediction, a model has been proposed and verified by experiments.

Acknowledgments

This work has been part of the ACEMU-project. The authors gratefully acknowledge the Danish Council for Strategic Research (1313-00004B) and EUDP (1440-0007) for providing financial support and would like to thank OXIS Energy for supplying the Lithium-Sulfur battery cells.

References

1. M. Wild, L. O'Neill, T. Zhang, R. Purkayastha, G. Minton, M. Marinescu, and G. J. Offer, *Energy Environ. Sci.*, **8**, 3477–3494 (2015).

2. D. Bresser, S. Passerini, and B. Scrosati, *Chem. Commun.*, **49**, 10545–10562 (2013).

3. P. A. Cassani and S. S. Williamson, *Conf. Proc. - IEEE Appl. Power Electron. Conf. Expo. - APEC*, 465–471 (2009).

4. S. Li, C. C. Mi, and M. Zhang, *IEEE Trans. Ind. Appl.*, **49**, 198–207 (2013).

5. J. V. Barreras, C. Pinto, R. De Castro, E. Schaltz, S. J. Andreasen, and R. E. Araújo, *2014 IEEE Veh. Power Propuls. Conf. VPPC 2014* (2015).

6. Y. H. Hsieh, T. J. Liang, S. M. Chen, W. Y. Horng, and Y. Y. Chung, *Power Electron. IEEE Trans.*, **28**, 5927–5939 (2013).

7. C.-H. Kim, M.-Y. Kim, and G.-W. Moon, *IEEE Trans. Power Electron.*, **28**, 3779–

3787 (2013).

8. Y. V. Mikhaylik and J. R. Akridge, *J. Electrochem. Soc.*, **151**, A1969 (2004).

9. D. Moy, A. Manivannan, and S. R. Narayanan, *J. Electrochem. Soc.*, **162**, A1–A7 (2014).

10. V. Knap, D. I. Stroe, R. Purkayastha, S. Walus, D. J. Auger, A. Fotouhi, and K. Propp, *ECS Trans.*, **77**, 479–490 (2017).

11. K. Propp, M. Marinescu, D. J. Auger, L. O'Neill, A. Fotouhi, K. Somasundaram, G. J. Offer, G. Minton, S. Longo, M. Wild, and V. Knap, *J. Power Sources*, **328**, 289–299 (2016).

12. V. Knap, D. I. Stroe, M. Swierczynski, R. Purkayastha, K. Propp, R. Teodorescu, and E. Schaltz, *J. Power Sources*, **336**, 325–331 (2016).

13. T. Zhang, M. Marinescu, S. Walus, and G. J. Offer, *Electrochim. Acta*, **219**, 502–508 (2016).

14. H. Schneider, T. Weiß, C. Scordilis-Kelley, J. Maeyer, K. Leitner, H. J. Peng, R. Schmidt, and J. Tomforde, *Electrochim. Acta*, **243**, 26–32 (2017).

https://dspace.org/

Self-balancing feature of Lithium-Sulfur batteries

Knap, Vaclav; Stroe, Daniel-Ioan; Christensen, Andreas E.; Propp, Karsten; Fotouhi, Abbas ...

2017-11-05
Elsevier
https://doi.org/10.1016/j.jpowsour.2017.10.078
Vaclav Knap, Daniel-Ioan Stroe, Andreas E. Christensen, Karsten Propp, Abbas Fotouhi, Daniel J. Auger, Erik Schaltz, Remus Teodorescu, Self-balancing feature of Lithium-Sulfur batteries, Journal of Power Sources, Volume 372, 2017, Pages 245-251

Downloaded from a DSpace repository. https://dspace.org/